Morphological and Spectroscopic Properties of Thin Films of Self-Assembling Amphiphilic Porphyrins on a Hydrophilic Surface as Revealed by Scanning Near-Field Optical Microscopy

Tetsuhiko Nagahara,[†] Kohei Imura,[†,‡] Hiromi Okamoto,*[,†,‡] Akane Oguro,[§] and Hiroshi Imahori*[,§,||]

Institute for Molecular Science and Graduate University for Advanced Studies, Myodaiji, Okazaki 444-8585, Japan, Department of Molecular Engineering, Graduate School of Engineering, Kyoto University, Katsura, Nishikyo-Ku, Kyoto 615-8510, Japan, and Fukui Institute for Fundamental Chemistry, Kyoto University, 34-4, Takano-Nishihiraki-cho, Sakyo-ku, Kyoto 606-8103, Japan

Received: June 15, 2005; In Final Form: August 16, 2005

We fabricated porphyrin thin films on mica surfaces from acidic aqueous solutions of the preorganized H-aggregates of amphiphilic porphyrins by the simple spin-coating method. The morphological and spectroscopic properties of the film were investigated by scanning near-field optical microscopy. The results obtained in this study demonstrate that the preorganized structure in solution can be transferred as a thin film with a thickness of the monolayer level without losing their substantial structure and photophysical properties.

1. Introduction

The incorporation of functional molecules into molecular devices requires deposition onto substrate surfaces in the form of thin film. The properties of the thin films thus obtained strongly depend on the structures of the molecules and their assembly. Not only the processibility but also the layer controllability is the key factor in fabrication of the films, since the properties of the ultrathin films are governed by their manner of assembly at molecular or mesoscopic scales.[1]

One convenient approach to make desirable thin films is the use of supramolecular interactions to assemble functional molecules. When noncovalent intermolecular interactions are introduced into functional molecules, they result in the controlled formation of mesoscopic structures. To adopt such mesoscopic structures to molecular devices, the supramolecular structures have to be supported on substrates without losing their structural and functional characteristics.[2] In this respect, we previously investigated photophysical properties of thin films that consist of quasi-one-dimensional porphyrin J-aggregates by scanning near-field optical microscopy (SNOM).[3−5]

In general, Langmuir−Blodget (LB) and spin-coating methods are commonly employed to form the thin films from solutions. A LB film, which is an ultimate thin monolayer film, shows an organized anisotropic structure and can be transferred to the substrate without losing the organized structure. Molecules used for the LB films are amphiphiles, which contain both hydrophilic and hydrophobic groups. If amphiphilic substituent groups are introduced in molecules that comprise a supramolecular structure, interaction between the supramolecule and the substrate surface may be expected.[6] On the other hand, controllability is limited for spin-coating, although it is known to be a good method in terms of processibility.[1]

Bearing these ideas in mind, we designed porphyrin molecules with amphiphilic groups at the *meso* positions, as shown in Figure 1.[7] *meso*-Tetraphenylporphyrins are known to form J- or H-aggregates in acidic aqueous solutions.[3−5,8−10] Such supramolecular structures would be stabilized in solution by introducing tetraalkylammonio groups including long alkyl spacers into the phenyl groups of *meso*-tetraphenylporphyrin, owing to van der Waals interactions between the alkyl spacers. More importantly, the cationic and hydrophilic tetraalkylammonio groups in the supramolecular structure are expected to interact well with anionic and hydrophilic surface (i.e., mica). In this paper, we report morphology and photophysical properties of the thin films of amphiphilic porphyrins on hydrophilic substrates, fabricated by spin-coating the preorganized porphyrin aggregate solution, as revealed by SNOM.

2. Experimental Section

Tetraalkylammonio-substituted porphyrins [5,10,15,20-tetrakis(4-(4-(trimethylammonio)butoxy)phenyl)porphyrin bromide (TABPP), 5,10,15,20-tetrakis(4-(8-(trimethylammonio)octyloxy)phenyl)porphyrin bromide (TAOPP), and 5,10,15,20-tetrakis(4-(12-(trimethylammonio)dodecyloxy)phenyl)porphyrin bromide (TADPP), Figure 1] and their reference compound without alkoxy moiety [5,10,15,20-tetrakis(4-trimethylammoniophenyl)porphyrin bromide (TAPP), Figure 1] were synthesized by following the same procedures as described in the literature (see Supporting Information S1).[7] Hereafter, we denote porphyrins in freebase and N-protonated (diacid) forms as H2C*n* and H4C*n*, respectively, where "*n*" denotes the number of carbon atoms in the alkyl chain [$n = 4$ (TABPP), 8 (TAOPP), 12 (TADPP)].

Hydrochloric acid (∼35%, reagent grade, Wako Pure Chemicals) was used without further purification. Distilled deionized water was purified by a water purification system (Milli-Q, Millipore). The sample solutions were prepared by dissolving a suitable amount of TABPP in water and adding hydrochloric

* To whom correspondence should be addressed. H.O.: fax, +81-564-55-4639; E-mail, aho@ims.ac.jp. H.I.: fax, +81-75-383-2571; E-mail, imahori@scl.kyoto-u.ac.jp.
† Institute for Molecular Science. E-mail: nagahara@cstf.kyushu-u.ac.jp.
‡ Graduate University for Advanced Studies.
§ Graduate School of Engineering, Kyoto University.
|| Fukui Institute for Fundamental Chemistry, Kyoto University.

10.1021/jp053220d CCC: $30.25
Published on Web 10/01/2005

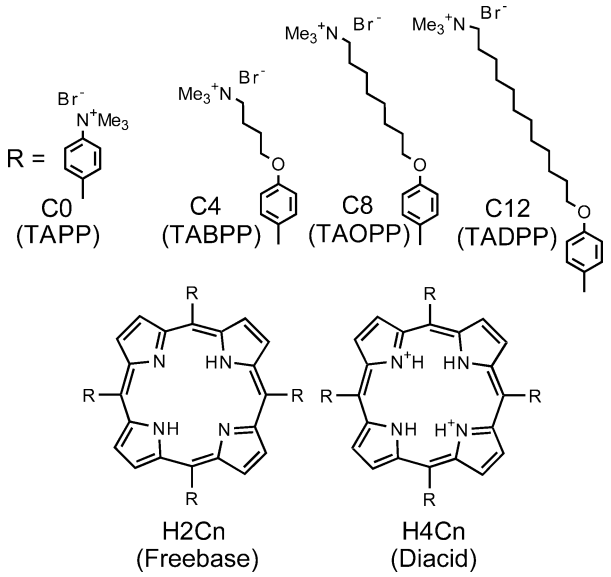

Figure 1. Molecular structures of porphyrins in freebase (H2C*n*) and diacid (H4C*n*) forms, where "*n*" denotes the number of carbon atoms in the alkyl chain ($n = 4$, 8, 12). The abbreviation "TABPP" has the same meaning as "H2C4" but is used for the starting material in the sample (solutions or thin films) preparation.

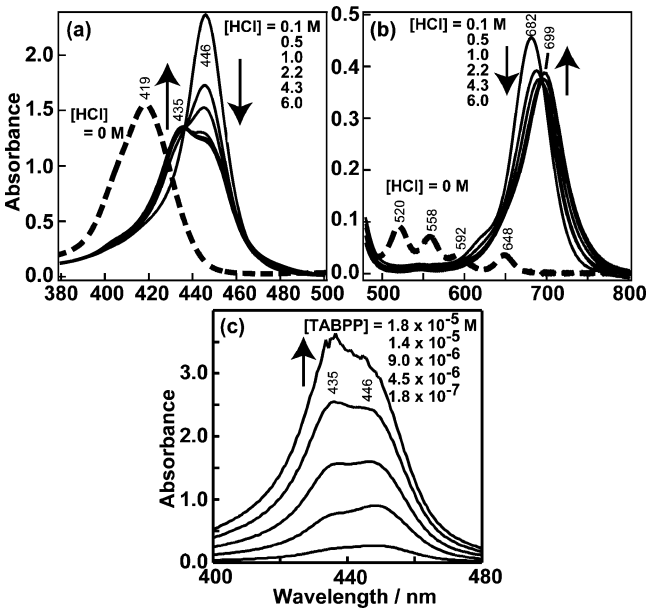

Figure 2. (a, b) Absorption spectral changes of TABPP (1.2×10^{-5} M) in water upon addition of HCl. Arrows indicate the direction of changes upon increasing the concentration of HCl. Freebase (H2C4) spectra, taken at [HCl] = 0 M, are also shown (dashed curves). (c) Absorption spectral changes of H4C4 in acidic water ([HCl] = 6.0 M) with increasing the TABPP concentration. Arrows indicate the direction of changes upon increasing the concentration of TABPP.

acid. Freshly cleaved mica was used as an atomically flat substrate. The acidic sample solution in water was spin-coated onto the mica substrate.

The details of the experimental setup are described elsewhere.[3] Briefly, the apparatus consists of an excitation light source, a home-built SNOM comprising a closed-loop *x*-*y*-*z* stage (nPoint), a microscope objectives (NA 1.2, Edmund Scientific), and detection systems. The second harmonics ($\lambda =$ 430 nm) of a mode-locked Ti:Sapphire laser (80 MHz, <100 fs, MaiTai, Spectra-Physics) was used as the light source. The near-field apertured probe used was a chemically etched gold-coated probe (aperture ~100 nm, NPU-102B, JASCO) made of a single-mode optical fiber. The averaged laser power incident on the fiber coupler was less than 0.5 mW. All the SNOM experiments were performed by applying the illumination (transmission) mode configuration. The distance between the aperture tip and the sample surface is regulated by the shear force feedback method. The feedback signal also gives the topographic image of the sample. The uncertainty of SNOM height measurements is less than 1 nm. The topography was also investigated by an atomic force microscope (AFM) with higher resolution (NanoScope IIIa, Digital Instruments, tapping mode in air).

For transmission measurements in the near-field, the light from the probe transmitted through the sample was detected by a photodiode after passing through appropriate filters, whereas fluorescence from the sample was detected by a polychromator (25 cm, CT-25TP, JASCO)/CCD (DV401-FI, Andor Technology) combination.

3. Results and Discussion

3.1. Aggregation in Water. As shown in Figure 2a,b (dashed curves), freebase H2C4 in water gives absorption maxima at $\lambda_{max} =$ 419, 520, 558, 592, and 648 nm whose spectral character is of the porphyrin with D_{2h} symmetry. At low HCl concentration ([HCl] = 0.1 M) in water, it forms the N-protonated diacid, H4C4 (D_{4h} symmetry), which exhibits absorption maxima at $\lambda_{max} =$ 446 and 682 nm, similar to that reported for 5,10,15,20-tetrakis(4-sulfonatophenyl)porphyrin (TSPP).[3−5,8−10] With further increase of the HCl concentration (0.5 M < [HCl] < 6.0 M), a new Soret band emerges at a shorter wavelength (435 nm) accompanied by a reduction of the diacid band (446 nm). Figure 2c shows a variation of the absorption spectrum as a function of TABPP concentration ([HCl] = 6.0 M). Again, a band at 435 nm becomes prominent with increasing dye concentration. A new species is formed at high concentration of HCl as well as the dye. The conversion of the diacid H4C4 to the new species in acidic solution is quantitative as indicated by two isosbestic points [437 and 694 nm in Figure 2a,b, respectively] below [HCl] ~ 1 M. The isosbestic point in the Soret region is blurred at a larger concentration than [HCl] ~ 1 M because of the slight spectral shift of the diacid band ($\lambda =$ 446, 448, 450, and 452 nm for [HCl] = 1, 4, 5, and 6 M, respectively).

It is well-known that stacked face-to-face aggregation leads to a blue-shift of the Soret band compared to the monomer (H-aggregate), whereas slipped face-to-face (or head-to-tail) aggregation leads to a red-shift (J-aggregate).[3−5,8,11,12] Since the new species shows a blue-shifted Soret band compared to the monomer and is generated only in high dye concentration the new species can be assigned as the H-aggregate of H4C4. Similar formation of the H-aggregates was also observed for the compounds with the longer alkoxy chains (H4C8 and H4C12). On the other hand, reference diacid H4C0, with no methyleneoxy spacer in the side group, revealed a slight red-shift of the Soret band with no isosbestic point with increasing concentration of HCl. These results support the significant contribution of the alkoxy spacer to stabilization of the H-aggregate as reported previously.[13] It should be noted that an addition of other concentrated acids (H_2SO_4 and HNO_3) to the aqueous solution of H4C4 did not exhibit the formation of the H-aggregate. This indicates that Cl^- anion is involved for the formation of the H-aggregate. Such effects of specific counteranions in aggregate formation were also reported previously.[9]

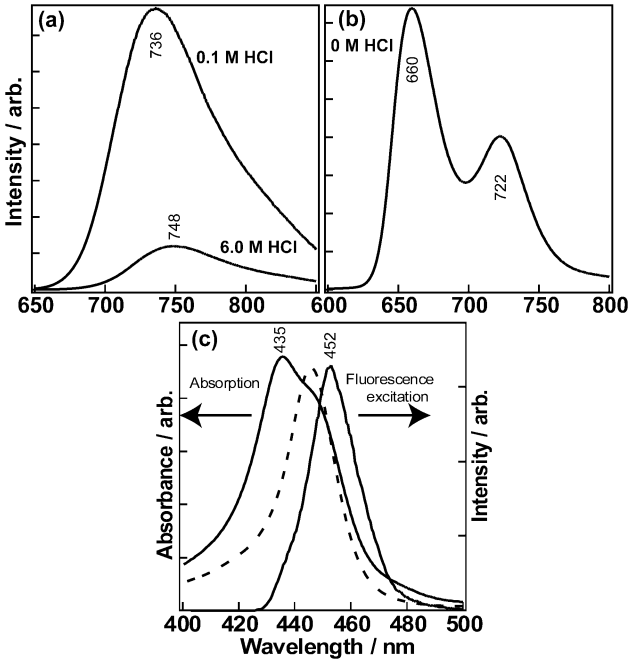

Figure 3. (a) Fluorescence spectra of TABPP in acidic water. (b) Fluorescence spectrum of TABPP in water. (c) Absorption and fluorescence excitation spectra of TABPP in acidic water ([HCl] = 6.0 M). The absorption spectrum of TABPP at [HCl] = 0.1 M is also shown (dashed curve).

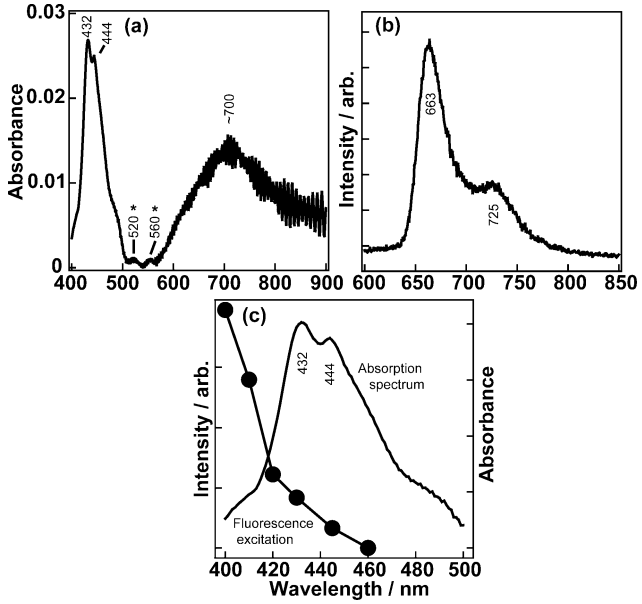

Figure 4. (a) Absorption spectrum of the thin-film sample of TABPP prepared by spin-coating the acidic ([HCl] = 6.0 M) solution on a mica substrate. Bands marked with an asterisk are not seen in the absorption spectrum in solution. See text for details. (b) Fluorescence spectrum of the TABPP thin-film sample on mica (excitation at 435 nm). (c) Fluorescence excitation spectrum (detection at 660 nm) and absorption spectrum of the TABPP thin-film sample on mica.

Figure 3a,b displays fluorescence spectra of diacid H4C4 and freebase H2C4, respectively, in water at the excitation of the Soret-band. As shown in Figure 3a, the diacid (H4C4) fluorescence showed a slight shift of the peak position and a significant reduction of the intensity with increasing concentration of HCl. Despite the considerable reduction of the fluorescence intensity, the fluorescence lifetime of diacid H4C4, as measured by the time-correlated single photon counting, is not significantly dependent on the concentration of HCl (τ = 1.78 ns, single exponential, at [HCl] = 6.0 M; τ = 2.13 ns, single exponential, at [HCl] = 0.1 M). In Figure 3c, the fluorescence excitation spectrum at high HCl concentration ([HCl] = 6.0 M) is compared with the absorption spectrum, together with the absorption spectrum of the monomeric diacid H4C4 [Figure 2a, [HCl] = 0.1M]. It is evident that the fluorescence excitation spectrum at the high HCl concentration is similar to the absorption spectrum of monomeric diacid (H4C4) solution rather than that at the high HCl concentration. The slight red-shift of the fluorescence excitation spectrum (at [HCl] = 6.0 M) compared to the absorption spectrum of monomeric H4C4 (at [HCl] = 0.1 M) is due to change in pH, which is also seen in Figure 2a ([HCl] > 1.0 M). Thus, it is concluded that the diacid (H4C4) monomer rather than the H4C4 H-aggregate is responsible for the fluorescence in water at the high HCl concentration ([HCl] = 6.0 M). The slight red-shift in the fluorescence spectra with increasing HCl concentration probably does not result from the H-aggregate formation but from the pH-dependent shift of the diacid monomer. The results obtained here reveal that in the highly acidic aqueous solution of H4C4 ([TABPP] = 1.5 $\times$ 10^{-3} M, [HCl] = 6.0 M), the absorption spectrum can be explained by the major presence of the H-aggregate, whereas the fluorescence can be accommodated by the minor presence of monomeric diacid H4C4. This conclusion is also consistent with the previous result on the decreased fluorescence quantum yield of the H-aggregate of TSPP diacid relative to that of the monomeric diacid.[14] In the following experiments we prepared the samples of the porphyrin thin films on substrates using an aqueous solution of the amphiphilic porphyrins at high HCl concentration.

3.2. Thin Film on Mica. The acidic aqueous TABPP solution ([TABPP] = 1.5 $\times$ 10^{-3} M, [HCl] = 6.0 M) was spin-coated onto mica. A typical absorption spectrum in the visible and near-infrared regions, after subtracting the absorption of the mica, is shown in Figure 4a. The periodic structure, in the wavelength region longer than ~600 nm, is due to the interference of light in the mica substrate. Bands at 432 and 444 nm in Soret region as well as a Q-band at ~700 nm are seen. These three bands are almost identical with those observed in the solution (Figure 2a,b), suggesting that the supramolecular H-aggregate structure is retained on the mica surface.

The fluorescence spectrum of the TABPP film on the mica is shown in Figure 4b. The spectrum is very similar to that of freebase (H2C4) in water (Figure 3b), which is in marked contrast to the diacid (H4C4) fluorescence observed in acidic water (Figure 3a). In particular, the fluorescence from the freebase porphyrin (H2C4) in water, as well as that from the TABPP film on the mica, reveals characteristic features of the porphyrin with D_{2h} symmetry, i.e., two peaks in the Q-band region (around 660 and 730 nm). This spectral similarity strongly suggests that the fluorescence from the TABPP film on the mica originates from a freebase-like species. In fact, in the absorption spectrum (Figure 4a), we can find very weak absorption bands, marked with asterisks, at ca. 520 and 560 nm. These two bands are very similar to those observed in freebase H2C4 in water (Figure 2b). The fluorescence excitation spectrum is compared with the absorption spectrum of the TABPP film on the mica (Figure 4c). The fluorescence excitation spectrum does not agree with the absorption spectrum of the TABPP film on the mica and any absorption spectrum of TABPP in water or in acidic aqueous solution (Figure 2). These results indicate an existence of a new absorption band in the shorter wavelength. In other words, a new species, which is not observed in solution, is formed on the mica substrate. The new species found in the sample on the mica may have an

TABLE 1: Major Components Observed in Absorption and Fluorescence Spectra of the Samples in Aqueous Solution and on Mica

	in pure water	in dil HCl	in conc HCl	on mica[a]
absorption	freebase monomer	diacid monomer	diacid aggregate	diacid aggregate
fluorescence	freebase monomer	diacid monomer	diacid monomer	freebase-like

[a] The acidic aqueous TABPP solution ([TABPP] = 1.5×10^{-3} M, [HCl] = 6.0 M) was spin-coated onto mica.

electronic structure similar to that of freebase H2C4, considering the fluorescence spectral characteristics (porphyrin of D_{2h} symmetry). The observed spectroscopic species in the solution as well as in the thin film are summarized in Table 1.

The freebase-like species under acidic conditions, found in the porphyrin thin film on the mica, are also observed in previous studies. Maiti et al. reported that freebase-like species were formed in the aqueous solution of *meso*-tetraphenylporphyrin at the high concentration (above the critical micellar concentration) of cetyltrimethylammonium bromide (CTAB) even under acidic conditions.[14] They ascribed the species to micellized monomer and explained that diacid underwent deprotonation to freebase form upon micellization even in acidic water because of hydrophobic environment inside the micellar regions. It may be noteworthy that CTAB is a hydrocarbon amphiphile with an ammonio group, similar to the substituent groups in the molecular structure of TABPP. Furthermore, the change in the electronic structure due to the adsorption of the porphyrin onto the substrate has to be considered. Iosif et al. reported that the fluorescence spectrum of tetrakis(4-methylpyridyl)porphyrin (TMPyP) molecules adsorbed on the inside surfaces of a quartz cell was distinct from that of the molecules in solution. An evolution of the fluorescence spectrum from the typical one for TMPyP to one with two peaks in the Q-band region was reported. They suggested that the change in the spectrum of the porphyrin on the adsorption results from vibronic mixing of the S_1 state with a nearby charge-transfer state.[15] Since it is less likely that such a CT state is formed in our sample without pyridyl moiety, deprotonated species may be more conceivable for the explanation of the monomer-like species found on the mica.

3.3. Microscopic Studies of Thin Film on Mica. AFM was used to evaluate the coating integrity of the thin film of TABPP on mica. The AFM image reveals the uniform smooth surface with some defects in the porphyrin film (Figure 5). We found a regular height of 3.0 nm, which corresponds almost exactly to one expected for the upright-standing porphyrin monolayer. An AFM image of H4C8, possessing the longer aliphatic side chains, on mica shows similar surface structure with some defects exhibiting a regular height of 3.5 nm. These regular heights are almost reproducible. Spin-coating on hydrophobic surfaces, such as Au(111) and HOPG, did not yield the similar smooth morphology on the surfaces. These results suggest that the electrostatic and hydrophilic interaction between the tetraalkylammonio group and the mica surface may facilitate the two-dimensional growth of the porphyrin films on the substrate during spin-coating.

The AFM image suggests the formation of monolayer porphyrins standing upright on mica substrate. In the visible and near-infrared absorption spectrum of the thin film (Figure 4a), the absorbance of the Soret band (~0.03) is comparable to that of upright-standing porphyrin monolayer on Au(111) and ITO surfaces (0.02−0.05) reported previously.[16,17] This observation also supports that the film is likely to be monolayer. We attempted to estimate the surface coverage as described in the following. The sample on the mica was resolubilized in the solvent, and the absorbance of the solution was measured. From

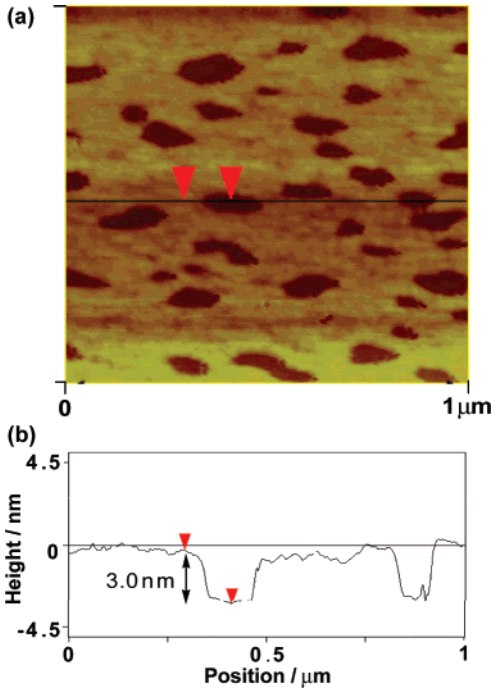

Figure 5. (a) AFM image of the thin film sample of TABPP prepared by spin-coating the acidic ([HCl] = 6.0 M) solution on mica substrate. (b) Section profile of the AFM image in (a).

the results, the number of the molecules on mica surface per unit area was estimated [$(4.6 \pm 0.3) \times 10^{17}$ molecules/m^2]. The mean molecular dimension of a TABPP molecule is assumed as $2.5 \times 2.5 \times 0.45$ nm^3. From the number density per unit area and the dimension of the molecule, the surface coverage was calculated by assuming the two different models on the molecular packing in the film: (1) face-to-face porphyrin aggregates in which the porphyrin plane lies vertical to the surface, where the molecule is attached to the substrate at one of the four side groups (covered area: 3.4×0.45 nm^2/molecule); (2) face-to-face stack of 6−7 porphyrin molecules, which give ~3 nm height, lying parallel to the surface (covered area: 2.5×2.5 nm^2 per 6−7 molecules). The surface coverage estimated in model 1 is ~70%, while that in model 2 is ~40%. Although both the models explain our AFM images in Figure 5, model 1 may be more plausible on the basis of the estimation. The layer heights estimated from the AFM images were not dependent on the rotation speed for the spin-coating of the solution or the concentration of the sample, which may also support model 1. As mentioned above, the thin film of H4C8 with longer aliphatic chain gives ~3.5 nm height, which again seems to be more reasonable for model 1. From these considerations, model 1 is more likely as the thin-film structure in the present system.

To characterize the properties of the thin film in mesoscopic scale, surface topography (Figure 6a) and transmission image (Figure 6b) at the H-aggregate band (λ = 430 nm) were measured by SNOM. The bright and dark parts in the transmission image correspond to high and low transmission intensities, respectively. The surface topography measured by SNOM was found to be similar to that obtained by AFM. These two images

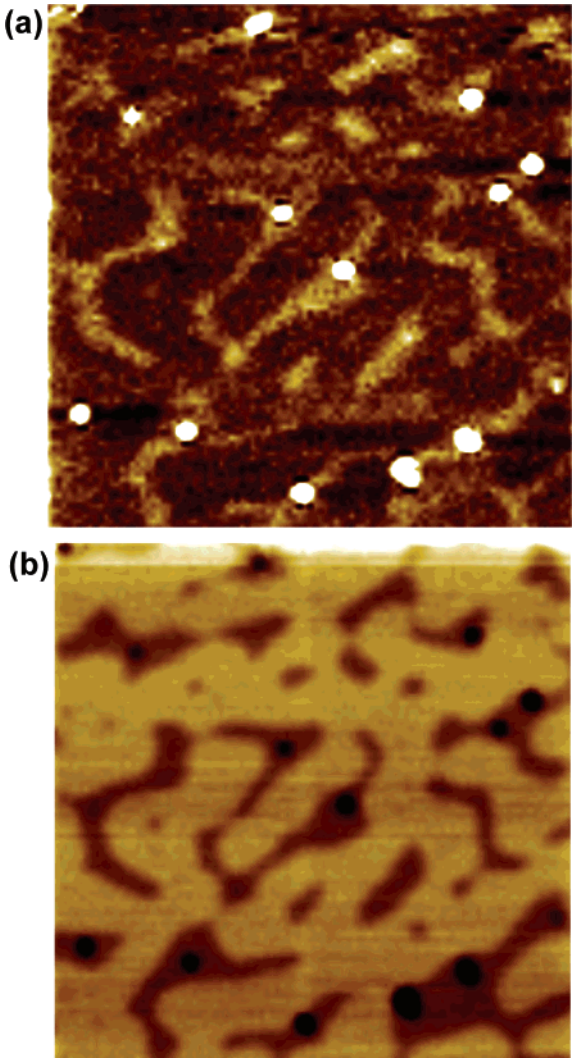

Figure 6. (a) Surface topography of the thin-film sample of TABPP on mica (scan area: 10 μm × 10 μm × 3 nm). Bright and dark parts correspond to high and low parts of the sample surface, respectively. (b) Transmission image of the sample obtained at 430 nm. Bright and dark parts correspond to high and low transmission intensities, respectively.

in Figure 6a,b are negatively correlated very well each other. That is, the optical transmission (at the H-aggregate band, 430 nm) at the position of higher topographic height (the bright part in the topographic image) is lower than that at the lower height position. This indicates that the film of ~3 nm height consists mainly of the H-aggregate. It should be noted here that the observed transmission image is not due to the topographic artifact[18] from the following evidence: the lateral position of the transmission image is sometimes shifted slightly compared to the topography when using a SNOM probe tip with a small protrusion outside the aperture, and the near-field transmittance change observed (~7%) is comparable to that for the far-field absorption of the porphyrin monolayer.

The fluorescence spectrum under the near-field excitation was also measured. Figure 7b,c displays fluorescence spectra (I_A, I_B, I_C, and I_D) at the positions specified in the topography (Figure 7a). The broad background signal, observed in the whole spectral region displayed, is due to luminescence from the optical fiber of the SNOM probe and from the mica substrate. The fluorescence from the sample, which consists of two bands (~650 and ~700 nm), is superposed on the broad background. The sample fluorescence is very similar to that observed in the far-field

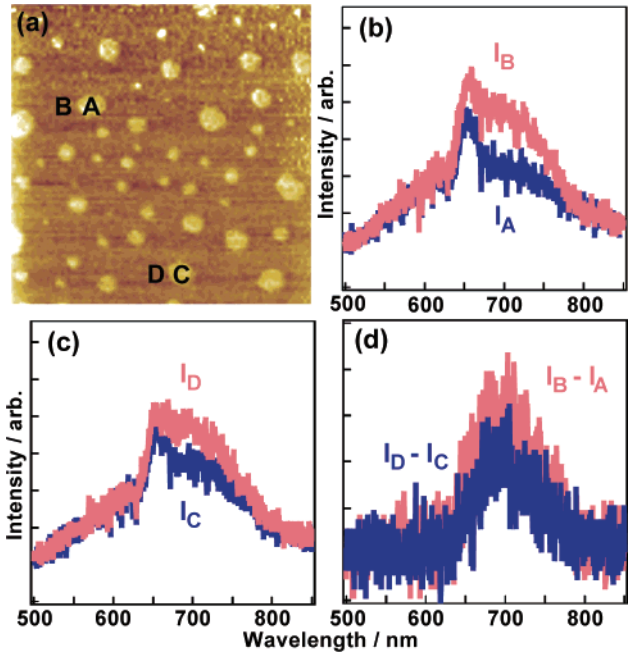

Figure 7. (a) Surface topography of the thin-film sample of TABPP on mica. Scan area: 5 μm × 5 μm × 4 nm. Bright and dark parts correspond to high and low parts of the sample surface, respectively. (b) Fluorescence spectra at position "A" (I_A) and at position "B" (I_B). (c) Fluorescence spectra at position "C" (I_C) and at position "D" (I_D). (d) Subtracted spectra, $I_B - I_A$ and $I_D - I_C$.

(Figure 4b) and is observed at all the positions, regardless of topographic height. This two-band structure disappears after photobleaching. From these observations, it seems more conceivable that the freebase-like fluorescent component, mentioned in the previous subsection, is formed when the free TABPP molecules are adsorbed on the mica surface. The fluorescent species is homogeneously spread over the mica substrate, whereas the nonfluorescent porphyrin molecules under the noncovalent interactions between the amphiphilic groups (i.e. H-aggregate) are more likely to be in the condensed part (positions "A" and "C").

Subtraction of the observed spectra, $I_A - I_B$ and $I_C - I_D$, gives a single band at ~700 nm (Figure 7d). This band is very similar to the H-aggregate absorption in the Q-band region shown in Figure 4a. This can be understood as the broad background luminescence from the SNOM probe being absorbed by the H-aggregate localized at the protruded part in the topography (i.e., positions "A" and "C"). The result in the Q-band region (~700 nm) is in good agreement with the transmission measurements at the Soret band (~430 nm, Figure 6). It should be noted here that spectra in A and C (and also B and D) are almost identical. Spectra in other protruded parts (and in other flat parts) are also very similar. This implies that such features do not largely originate from inhomogeneous environmental effects.

4. Concluding Remarks

The results obtained in this study demonstrate that the preorganized H-aggregate of amphiphilic porphyrin in aqueous HCl solution can be successfully transferred onto mica substrates as a thin film with a level of monolayer, without losing their mesoscopic structure and photophysical properties. Although the question of exact molecular orientation on the surface remains open in the present stage, our methodology will open a door for the fabrication of self-organizing porphyrin on

surfaces, which exhibit novel structure and photophysical function.

Acknowledgment. This study was partly supported by Grants-in-Aid (No. 16350015 to H.O. and No. 16310073 to H.I.) from Japan Society for the Promotion of Science. H.I. also is thankful for the Grant-in-Aid from MEXT of Japan (21st Century COE on Kyoto University Alliance for Chemistry) for financial support. We thank Dr. Yasuyuki Araki and Prof. Osamu Ito of Tohoku University for the fluorescence lifetime measurements.

Supporting Information Available: Synthesis of amphiphilic porphyrins and their reference compound (S1). This material is available free of charge via the Internet at http://pubs.acs.org.

References and Notes

(1) *Functionality of Molecular Systems*; Honda, K., Ed.; Springer-Verlag: Heidelberg, Germany, 1998.

(2) *Chemistry of Nanomolecular Systems: Towards the Realization of Nanomolecular Devices*; Nakamura, T., Matsumoto, T., Tada, H., Sugiura, K.-i., Eds.; Springer-Verlag: Heidelberg, Germany, 2003.

(3) Nagahara, T.; Imura, K.; Okamoto, H. *Chem. Phys. Lett.* **2003**, *381*, 368.

(4) Nagahara, T.; Imura, K.; Okamoto, H. *Rev. Sci. Instrum.* **2004**, *75*, 4528.

(5) Nagahara, T.; Imura, K.; Okamoto, H. *Scanning* **2004**, *26*, I10.

(6) Yao, M.; Iwamura, Y.; Inoue, H.; Yoshioka, N. *Langmuir* **2005**, *21*, 595.

(7) Mukundan, N. E.; Petho, G.; Dixon, D. W.; Kim, M. S.; Marzilli, L. G. *Inorg. Chem.* **1994**, *33*, 4676.

(8) Ohno, O.; Kaizu, Y.; Kobayashi, H. *J. Chem. Phys.* **1993**, *99*, 4128.

(9) Okada, S.; Segawa, H. *J. Am. Chem. Soc.* **2003**, *125*, 2792.

(10) Rosa, A.; Ricciardi, G.; Baerends, E. J.; Romeo, A.; Scolaro, L. M. *J. Phys. Chem. A* **2003**, *107*, 11468.

(11) Kano, K.; Fukuda, K.; Wakami, H.; Nishiyabu, R.; Pasternack, R. F. *J. Am. Chem. Soc.* **2000**, *122*, 7494.

(12) Osuka, A.; Maruyama, K. *J. Am. Chem. Soc.* **1988**, *110*, 4454.

(13) Elangovan, T.; Krishnan, V. *Chem. Phys. Lett.* **1992**, *194*, 139.

(14) Maiti, N. C.; Mazumdar, S.; Periasamy, N. *J. Phys. Chem. B* **1998**, *102*, 1528.

(15) Iosif, A.; Grummt, U.-W. *J. Prakt. Chem.* **1997**, *339*, 420.

(16) Imahori, H.; Hosomizu, K.; Mori, Y.; Sato, T.; Ahn, T. K.; Kim, S. K.; Kim, D.; Nishimura, Y.; Yamazaki, I.; Ishii, H.; Hotta, H.; Matano, Y. *J. Phys. Chem. B* **2004**, *108*, 5018.

(17) Yamada, H.; Imahori, H.; Nishimura, Y.; Yamazaki, I.; Ahn, T. K.; Kim, S. K.; Kim, D.; Fukuzumi, S. *J. Am. Chem. Soc.* **2003**, *125*, 9129.

(18) Valaskovic, G. A.; Holton, M.; Morrison, G. H. *J. Microsc.* **1995**, *179*, 29.